Climate Change Projections of Sea Level Extremes along the California Coast

Daniel R. Cayan[1,2], Peter D. Bromirski[1], Katharine Hayhoe[3], Mary Tyree[1], Michael D. Dettinger[2,1], and Reinhard E. Flick[4,1]

1 Scripps Institution of Oceanography, University of California, San Diego
2 U. S. Geological Survey, Water Resources Division
3 Texas Tech University, Dept. of Geosciences
4 California Department of Boating and Waterways

Abstract. California's coastal observations and global model projections indicate that California's open coast and estuaries will experience rising sea levels over the next century. During the last several decades, the upward historical trends, quantified from a small set of California tide gages, have been approximately 20 cm per century, quite similar to that estimated for global mean sea level. In the next several decades, warming produced by climate model simulations indicates that sea level rise could amplify. Rates projected could exceed substantially the rate experienced during modern human development on the California coast and estuaries. A range of future SLR is estimated from a set of climate simulations governed by lower (B1), middle-upper (A2), and higher (A1fi) GHG emission scenarios. Projecting SLR from the ocean warming in GCMs, observational evidence of SLR, and separate calculations using a simple climate model yields a range of potential sea level increases, from 11 cm to 72 cm, by the 2070-2099 period. The combination of predicted astronomical tides with projected weather forcing, El Nino related variability, and secular SLR, gives a series of hourly sea level projections for 2005-2100. Gradual sea level rise progressively worsens the impacts of high tides and the surge and waves associated with storms, and also freshwater floods from Sierra and coastal mountain catchments. The occurrence of extreme events, relative to current

levels, follows a sharply escalating pattern as the magnitude of future sea level rise increases.

1 Introductuion

California has about 1800km of coastline, numerous estuaries including the San Francisco Bay and Delta, wetlands, and coastal aquifers. These are susceptible to harmful effects if sea level rises too much or too fast in the 21st Century.

For at least the past 20,000 years, sea level has been rising at various rates as a result of the last and ongoing episode of global warming and related glacial and icecap melting and retreat. (Fairbanks 1989).   During the most rapid period of rise from about 18,000 to about 5,000 years ago, sea level rose nearly 120 meters (almost 400 feet), or an average of about 1 meter per century. Sea level is estimated to have risen at an average rate of about 5 cm per century during the past 6,000 years, and at an average rate of 1 to 2 cm per century during the past 3,000 years (Church et al. 2001). These rates have been reflected along California's coastline.

During the 20th Century, from a collection of tide gages, global sea level rose an estimated 1.8mm/yr (Church et al. 2001), and during the recent 1993-2003 period, from satellite altimetry, global sea level has risen approximately 2.8mm/yr (Cazenave et al. 2004) . Identifying sources of the global rise leaves a conumdrum, in that estimates of the two predominant sources, steric increases in ocean volume due to thermal expansion and eustatic increases due to melting of ground-based ice only accounts for about half of this estimated increase (Munk 2002; Cazenave et al. 2004). Tide gauge records in California and other west coast United States locations that are tectonically stable (Figure

1) show corresponding rises (although the correspondence may be chance). Sea-level rise (SLR) along the West Coast has been more or less continuous during the 20th Century , but has been marked by considerable interannual and decadal variability (Bromirski et al. 2003). Interestingly, the records in Figure 1 do not indicate recent increases in the rates of SLR, but rather have been relatively flat since about 1983. However, viewed over the longer term, SLR has been an important component of sea level along the entire California coast. The occurrence of extremes has increased markedly (Table 1), e.g., at San Francisco (by 20-fold since 1915) and at La Jolla (by 30-fold since 1933).   If sea level continues to rise, these extremes will become even more common.

This paper provides an evaluation of possible evolution and properties of 21st Century sea-level extremes, consistent with climate-change projections described elsewhere in this volume.

2   Short-period Variations of California Sea Level

The SLR discussed above are embedded in an envelope of short-term sea-level fluctuations that determine how and when most sea-level extremes occur. Most of the "spread" in the distribution of sea levels is caused by tides, e.g. regular changes of ocean water levels caused by the gravitational forces of the moon and sun. Tides are the largest components of sea level change, with open coast tide ranges in California of up to about 3 m, trough to peak (Table 1). Tides are the only component of sea-level variability that are accurately predictable.

The most important tidal time scales on the California coast are semidiurnal, diurnal, semi-monthly, semiannual and 4.4 years. California's tide regime is distinctly

different from the semi-diurnal conditions that dominate the east coast of the United States. On the California coast, tides are mixed, periodically having nearly equal semi-daily and daily components (Zetler and Flick, 1985).   The monthly tidal changes are dominated by the spring-neap cycle, with two periods with large tidal ranges (springs) near the times of full and new moon, and two periods with lower ranges (neaps) near times of the quarter moons. One spring tide range per month is usually higher than the other, a consequence of the moon's distance and declination. As a result of lunar and solar declination effects, highest monthly tides in the winter and summer months are higher than those in the spring and fall, with their respective differences ranging up to about 0.5 m. Furthermore, the extreme monthly higher-high tides in the winter tend to occur in the morning, sometimes quite early (Flick 2000). On the California coast, the distinct 4.4-year cycle results in higher peak monthly tides of about 0.15 m, compared with years in between. This cycle peaked in 1982–1983, 1986–1987, 1990–1991, 1995–1996, and 1999–2000, etc.

Other less predictable fluctuations also contribute to local sea level changes, including storm surges, large scale changes in water temperature and wind forcing, and climate related fluctuations (Flick 1998). Storm surge is that portion of the local, instantaneous sea level elevation that exceeds the predicted tide and which is attributable to the effects of low barometric pressure and high wind associated with storms. Storm surge along the California coast, excluding the effect of waves, rarely exceeds 0.3 m in amplitude (Flick and Badan-Dangon 1989; Flick 1998). However, wave induced surge on a beach can be of the order of the significant breaker height, which can reach 1.5 m or more. During El Ninos, large scale oceanic and atmospheric mechanisms often elevate

sea level along the West Coast (Chelton and Davis, 1982; Flick 1998; Seymour et al. 1984; Seymour, 1998; Storlazzi and Griggs, 1998; Bromirski et al. 2003), yielding non-tide sea-level anomalies with amplitudes of several cm that may persist for several months.

3   Projections of Global Sea Level Rise

Over the next few hundred years, global sea level is expected to rise because, at present, the earth's radiation budget is out of balance (Hanson et al. 2005) and the earth, especially the oceans, is still heating (Wigley 2005; Meehl et al. 2005) and because, in the foreseeable future, projected increases in greenhouse gases and associated increases in temperature (Church et al. 2001). SLR of several cm is likely from thermal expansion of sea water, but it could reach several meters from melting of continental ground-based ice, especially in Greenland and Antarctica (Alley et al., 2005). Because the historical rate of SLR at California tide gages is quite similar to the estimated global rate, future SLR in California is expected to follow global SLR.

Projected ranges in SLR due to thermal expansion (TE) are a natural outgrowth of recent projections of warming over the next century, and are available from climate simulations of the IPCC SRES A2 and B1 greenhouse-gas (GHG) emissions scenarios. However, SLR due to land-ice melt (IM) is not yet for a part of the latest projections. Because ice melt is an important component of global SLR (Church et al. 2001, Cazenave et al. 2004), an accounting of the land-ice contributions is necessary to estimate overall SLR. For a guideline of likely or possible sea level rise in California during the next century, we use the TE component from the GCM's together with the MAGICC "simple

climate model" (Hulme et al. 1995; Wigley 2005) to derive sea level changes over the 100 year projection. The starting point of this model exercise uses as an initial value the relative contributions of TE and IM. The model then calculates, stepping forward in time, the amount of SLR, including its TE and IM components. Because of the uncertainty in the relative fraction of these two components, the MAGICC calculation is repeated using three (high, medium, and low) estimates of IM vs. TE, as shown in Figure 2. SLR projections for the A1fi scenario (high greenhouse gas emissions) were not available from the climate models analyzed in the present study. Therefore, A1fi values of TE were estimated from A1fi simulations by previous models, based on the differences between A2 projections from those previous models and the current A2 projections. The IM contribution was then estimated by the approach described above.

A superposition of the associated SLR estimates corresponding to the different GCM and emission scenario simulations produces an envelope of possible sea level rise from 2000-2100, shown in Figure 3. By mid-century (2035–2064), projections of global SLR range from ~6-32 cm above 1990 levels, with no discernable inter-scenario differences, as shown in Figure 3 and Table 2. By end-of-century (2070–2100), however, SLR projections range from 10–54 cm under B1, to 14–61 cm under A2, and 17–72 cm under A1fi.

4   A Model of Hourly Sea Levels

To determine the likely influence of SLR (and other climate changes) on the future statistics of extreme sea levels, a model of hourly sea level variations at three

California coastal tide gage stations (Crescent City, San Francisco, and La Jolla) was developed. The model includes the following components (a-d below):

a) Astronomical tides are predicted with good precision based on known tidal constituents (Zetler and Flick, 1985; Munk and Cartright 1966) and a typical tidal prediction program developed by Munk (personal communication) and his co-workers at Scripps Institution of Oceanography. The standard tidal harmonic information published by NOAA on their website was used for each location. This consists of between about 20 and 30 constituents with amplitude and phase values derived from past observations. Corrections for apparent secular increases in the amplitude of the tide were not included (Flick et al. 2003).

b) Sea level fluctuations due to barometric (sea level pressure, SLP) and wind stress fluctuations were modeled using linear regression equations relating historical non-tidal sea level residuals from predicted tide heights, to local SLP and offshore wind stresses from the NCAR/NCEP Reanalysis dataset, 1950–2004 (Kalnay et al. 1996) The greatest influence on short period non-tide sea level variability is that from inverse barometer effects, with wind stress contributing only incrementally. Time series of 21st Century SLP and wind stresses were extracted from each of four atmosphere-ocean general circulation model (GCM) simulations: A2 and B1 scenarios simulated by the NOAA Geophysical Fluids Dynamics Laboratory (GFDL) CM2.1 model (Delworth et al. 2006) and by the National Center for Atmospheric Research (NCAR) Parallel Climate Model (PCM) (Washington et al. 2000). (Because SLR projections from each of several simulations were similar, only results from the GFDL A2 simulation are shown here.)

SLP simulated by the models has mean and variance that are in good agreement with SLP from the NCEP Reanalysis. The sea-level model was applied at hourly intervals in order to capture synoptic variability, but because the climate projections and Reanalysis were only available at daily, not hourly, intervals, additional disaggregation of the inputs was required. To synthesize hourly SLP, a day-long sequence of hourly SLP observed at airport weather stations was interjected around each simulated day's daily mean, with requirements that: (1) the mean daily SLP from the weather station was within 8 hPa of the projection's daily mean, and (2) the first hour of a given day's SLP matched the last hour of the preceding day's SLP within 4 hPa in order to retain a relatively realistic and smoothly varying SLP predictor. Hourly wind stress variations were generated using simple linear interpolation between the daily mean values from the GCM, centered at mid-day.

c) Monthly-to-interannual sea-level fluctuations associated with El Nino/Southern Oscillation (ENSO) contribute the dominant part of sea level variability at seasonal-interannual time scales. The ENSO component was incorporated using a simple regression equation relating monthly NINO 3.4 SSTs (averaged over 120ºW–170ºW, 5ºS–5ºN) to smoothed observed sea levels at California's tide stations. Assuming that the same mechanisms operate in the future, ENSO variability was extracted from the climate simulations as detrended NINO 3.4 SSTs, which were rescaled to match the standard deviation of the observed Nino 3.4 series for 1961–1990. In the GFDL CM2.1 simulations, this NINO 3.4 SST index was well correlated with another commonly used ENSO index, the Southern Oscillation Index; correlation coefficients were -0.65 for monthly data, September through February; and -0.82 for seasonal mean data from the

GFDL CM2.1 2005-2099 A2 simulation. Using these projected NINO 3.4 values, the corresponding ENSO-induced sea-level fluctuations for California were projected using the historical regression relation. Because the ENSO and weather components were extracted from the same climate model sequences at known points in (future) time, the simultaneity of the ENSO, weather, and tidal contributions was ensured. Two other North Pacific climate indices, NP (Trenberth and Hurrel 1994) and PNA (Wallace and Gutzler 1981), did not account for significant fractions of variance of the sea level anomaly at the three coastal stations, so they were not included as predictors.

d) Finally, mean SLR was obtained from Figure 3. To cover the range of potential SLR, a set of linear rates from +10 to +80 cm per hundred years were added to the short term sea-level components.

Simulated sea level anomalies and resultant total sea level height is shown in Figure 4 for a two month period during winter 2006 San Francisco. The variability of the simulated sea level anomaly series resembles that from the observed sea level anomaly. There is also good correspondence between the magnitude and temporal variations of the monthly average simulated sea level and that from historical observations, as shown in Figure 5 for 2000–2100 GFLD simulated series in comparison to 1900-2000 observed sea level from the San Francisco record. Other simulations constructed from the GFDL CM2.1 B1 emissions scenario and from PCM A2 and B1 emissions scenarios, produced quantitatively similar results as those for the GFDL CM2.1 A2 simulation, so they are not shown here.

The regression relations and fits developed from observed sea levels at Crescent City, San Francisco, and La Jolla are reported in Table 3. The model replicates approximately 50% of the historical daily mean sea level height anomaly variance using three relatively simple weather inputs: SLP, zonal, and meridional wind stress components. The overall fraction of variance of the non-tidal sea level anomalies, not including the variability introduced by the long period trend, ranged from 68% at Crescent City to 45% at La Jolla, as shown in Table 3. The variability in the linear model is of similar magnitude, but somewhat smaller than that in the observations, with model standard deviations ranging from 82% (Crescent City) to 66% (La Jolla) of those of the observed sea level daily non-tide anomalies. SLP provided the dominant fraction of the explained variance; only about 10% was explained by the wind stress components. A reasonable fraction of the monthly to interannual variability of sea level anomaly was explained by Nino 3.4, with approximately 5 cm of sea level per ºC of Nino 3.4 SST anomaly, meaning that a significant El Niño having +2ºC SST anomaly will raise sea level at the coastal stations by about 10 cm.

5 Projected Sea Level Extremes

Climate change is likely to raise mean sea levels, which would lead to inundation of some low-lying areas and adversely affect coastal aquifers. However, some of the most serious impacts would result from the extreme sea levels associated with tides, winter storms, and other episodic events that would be perched upon higher baseline sea level. Extreme high water levels (measured by any fixed threshold) would occur with increasing frequency (i.e., with shorter return period) as a result of mean SLR. Many

California coastal areas are at risk from sea level extremes, especially in combination with winter storms (Flick 1998). During the 1997–1998 El Niño, very high seas and storm surge caused hundreds of millions of dollars in storm and flood damage in the San Francisco Bay area. Highways were flooded as six-foot waves splashed over waterfront bulkheads, and valuable coastal real estate was destroyed (Ryan 2000).

The frequency of high sea level extremes also may be increased if storms become more frequent or severe as a result of climate change. Increases in the duration of high storm-forced sea levels increases the likelihood that they will occur during high tides. The combination of severe winter storms with SLR and high tides would result in extreme sea levels that could expose the coast to severe flooding and erosion, damage to coastal structures and real estate, and salinity intrusion into delta areas and coastal aquifers.

Not surprisingly, then, projected sea level extremes become more common as sea level rises. There is a marked increase of sea level extremes as sea level increases (*a*) over the 21st century, and (*b*) as the imposed SLR rate is increased from zero to 80 cm over the 100-year period. Table 4 describes how, at San Francisco, with +30 cm/century rate of rise, the occurrence of events above it's historical (1960-1978) 99.99 percentile of 141cm above mean sea level increases from just less than one hourly event in one year to about 1.3 events per year averaged over 2005-2034, to about 7 events per year during 2035-2064 to about 17 events per year in 2070-2099. If, instead, the rate of SLR is 60 cm/century, the incidence of hourly events exceeding the historical 99.99 percentile climbs to 4.6 per year during 2005-2034, to about 41 per year during 2035-2064, and to about 235 per year during 2070-2099. Similar increases in the occurrence of

extremes with hypothetical sea level rise are found in the modeled sea levels at La Jolla and Crescent City (not shown).

The influence of weather events and ENSO in producing high sea level extremes is evidenced by two additional runs of the statistical model, one with no weather and one with no weather and no ENSO input, shown in Table 5. The "no weather, no ENSO" simulations indicate that these natural fluctuations are required to produce virtually all of the hourly sea level exceedances above the historical (1960-1978) 99.99 percentile threshold. When the largest (80 cm/100yr) SLR rates are imposed and as time progresses, these exceedances become more and more prevalent, until, with the largest trends during the 2070–2099 period, the number of exceedances from "no weather, no ENSO" reach almost the same level as those produced by the "full" model of weather, ENSO, tide and trend components. The "no weather" simulations indicate that synoptic scale (a few days) weather disturbances play a critical role in generating extremes, with more than half of the 99.99 percentile level exceedances during the historical period eliminated during the "no weather" run. On the other hand, these results also illustrate the key role played by ENSO in producing sea level extremes, as the exceedances that remain can be attributed to ENSO effects.

Considering the ranges of SLR expected from the three emissions scenarios (Figure 3), if warming is modest so that SLR rates are at the low end of each emissions scenario, the increases in extreme events would increase, but not greatly, and temperatures, SLR and sea-level extremes from the three scenarios (B1, A2, A1fi) would not be that different from each other. On the other hand, if warming is large so SLR values are at the higher end of each emissions scenario, the incidence of extreme events

would increase markedly and the three scenarios (B1, A2, A1fi) would be sharply differentiated. In this case, the highest emission scenario would produce a much greater occurrence of high sea level events, and the question of which emissions scenario we will most nearly replicate determines how much greater.

In addition to its effects on the open coast, SLR and attendant inundations may have severe impacts on low-lying land bordering the San Francisco Bay and Delta. This would damage marginal ecosystems as well as degrading the quality and reliability of the fresh water supply pumped from the southern edge of the San Francisco Delta. Inundation would be worsened when high sea levels are exacerbated by freshwater floods. To explore this, Figure 6 shows—for the San Francisco (SFO) sea-level scenario based on the GFDL climate under A2 emissions and with an assumed sea-level trend of 30 cm/century—the counts of hours per year with SFO sea levels above the 99.99% historical sea-level range (in black). Also shown are corresponding counts of high sea-level stands that co-occurred when the simulated SFO sea-level pressure (SLP) was low enough to threaten stormy/wet weather. To estimate this SLP threshold, daily SLPs were regressed against daily flows in the North Fork American River during November-March from 1949–1999 to quantify how SLP levels correspond to various flow levels in central Sierra Nevada Rivers. The 90 historical days with largest flows in the North Fork American River (average of 2/yr, top 0.5% of observed flows) were identified, and from those flows, a historical 99.5% exceedance level for flows in the American River was estimated. The SLP threshold corresponding to that flow threshold was then estimated from the flow-SLP regression equation (-4 mb). Using this SLP threshold, the number of hours per year during which both (a) sea levels exceeded the 99.99% threshold and (b)

the SLP values were lower than the SLP threshold were plotted (Figure 6, in red). The sequences shown indicate that, under the 30cm/century SLR rate, the storm/high-sea level coincidences increases at least until about mid-century and, indeed, makes up most of the increasing numbers of sea-level threshold exceedances until then. Sometime near mid-century, the number of coincidences saturates (becomes more or less stable but still much more common than in the historical period or early decades of the 21st century) and the total number of sea-level exceedances, not associated with low SLPs, continues to grow. As indicated earlier, synoptic scale weather disturbances are critical contributors to the observed and projected sea-level extremes, at least until SLR has markedly raised the base levels from which other influences generate extremes. In the Bay and Bay-ward parts of the Delta, this sequence of new sea-level exceedances suggest that the number of opportunities for high-sea-level stands and floods to coincide may increase most rapidly in the early-to-middle stages of 21st century sea-level rise.

6 Waves and Sea Level

Most coastal damage in California occurs during periods when both extreme sea levels and extreme wave heights occur simultaneously (Flick 1998). The additional impact that waves may add to high coastal sea levels can be characterized probabilistically, recognizing that wave amplitudes are related to storminess, which is related to sea level anomalies. In the PCM and GFDL model projections employed here, storminess along the California coast is marked by interannual and decadal variability, similar to the last several decades of various instrumental records (Bromirski et al. 2003 and Figure 7, lower), but shows little tendency for a secular change over the 21st Century,

as shown by the incidence of low sea level pressure events plotted in Figure 7, upper. The relationship between significant wave height (Hs; defined as the average height of the one-third highest waves) and non-tidal sea levels can be described using historical wave buoy and sea level records in Northern California (near Crescent City), Central California (near San Francisco), and Southern California (near La Jolla), from approximately 1981–present. Extreme wave heights and extreme non-tide sea level fluctuations tend to increase from the south to the north along the California coast, demonstrated by Gaussian probability distributions of the ranked estimates (Figure 8). The most dramatic change, moving northward along the coast, is the large increase in wave heights (Figure 8, top) between Pt. Conception (SCA, green) and San Diego (SIO, blue), with San Diego shielded—along with the rest of the Southern California Bite coastline--by Pt. Conception and the Channel Islands. Differences in the wave energy probability distributions between Pt. Conception and locations farther north, near San Francisco (CCA) and Crescent City (NCA), are small, except only for the most extreme waves. The similarity of wave heights north of Pt. Conception reflects the fact that, to the north, a dominant mode of wave height variability is shared all along the central and northern California coasts (Bromirski et al. 2005).

Extreme sea level height fluctuations are also larger to the north, as a result of increasing storm intensities at the more northerly coastal locations (Figure 8, bottom). The non-tide sea levels are obtained by spectrally removing the tidal energy from the hourly tide gauge records (Bromirski et al. 2003). Note that, for example, a 30 cm event is much less likely near San Diego (SIO) than near either San Francisco (SFO) or Crescent City (CRE).

The probabilities of the potentially important co-occurrences of extreme waves and extreme sea level heights are illustrated for peak Hs's at NOAA buoys near San Francisco in Figure 9. The probability distribution in Figure 8 shows the historical (1981-present) frequencies of occurrences of peak Hs's during times when the non-tide sea level heights were continuously above the 25th, 50th, 75th, 95th, and 99th percentile thresholds for at least three hours, respectively. The resulting distributions indicate that higher Hs's are more likely during higher anomalous non-tide sea-level stands than during lower sea-level anomalies. For example, the most likely value of peak Hs rises from about 2.5m to over 5m, as non-tide sea level anomalies increase from 4cm to 30cm. This reflects the important role of storms in driving, often simultaneously, high sea levels and high waves.

Summary

Coastal observations and global climate projections indicate that California's coast will experience rising sea levels during the 21st century. Sea level rise (SLR) projected using output from recent global climate model runs increases in proportion to the amount of global warming. By 2070–2099, projected SLR ranges from 13 to 76 cm, depending on the magnitude of climate warming (which is generally larger for scenarios with higher projected greenhouse gas concentrations. The middle to higher end of this range would substantially exceed the historical rate of sea level rise, approximately 20 cm per century, observed at San Francisco and San Diego during the past 100 years.

Problems created by SLR are greatly aggravated by higher frequency sea level phenomena. In particular, sea-level extremes are even more dangerous in many settings than are the long-term mean rises themselves, and the extremes occur when the long-

term changes coincide with shorter period fluctuations These other higher frequency fluctuations derive from tides, weather, and climatic fluctuations such as El Nino/Southern Oscillation events. The present study considers output from two climate models (GFDL and PCM) and three emission scenarios to provide a set of future weather and short period climate fluctuations, and a range of potential long-term sea level rises. Using a model of the combined contributions to hourly sea level of predicted tides and model-simulated weather, climate, and long-term global warming, the potential for SLR– induced changes in the occurrence of hourly extremes was assessed. If sea level rise trends are near the low end, the occurrence of extremely high-sea level events will increase, but the increase in extremes would be not so different from the increase in extremes that has been experienced along the California coast during the last several decades, as outlined in Table 1. On the other hand, if sea level rises climb to the higher end, extreme events and their duration would increase markedly, substantially beyond any recent increase during California's 19th and 20th Century human experience.

Coastal sea level extremes are also exacerbated by other storm effects, such as heavy surf from wind-driven waves. Implications are that when short term anomalous sea level is highest, wave energy has an increased likelihood of reaching very high levels When these factors coincide with high tides, the chances for coastal damage are greatly heightened. Continuing increases in mean sea level due to global change makes this problem ever more severe.

In the San Francisco Bay estuary, sea level rise effects may be compounded by riverine floods that feed into the northern reaches of the Bay from the Sacramento/San Joaquin Delta. Storms are important causes of the highest water levels both because of

the barometric and wind effects on the sea levels that accompany them, and because of the (freshwater) floods that they can generate. As climate warms, snow levels rise, and snowmelt comes faster, the Sierra Nevada watershed would generate rapid (storm-time) runoff over a larger range of elevations. The combination of flood and high sea-level stands are particularly dangerous in the Delta, where the combination of sea level and river stages determine water heights.

References

Alley, RB, Clark, PU, Huybrechts, P., and Joughin, I., 2005: Ice-sheet and sea-level changes. Science, v. **310**, p. 456-460.

Bromirski, P.D., D.R. Cayan, and R.E. Flick, 2005: Wave spectral energy variability in the northeast Pacific, *J. Geophys. Res.*, **110**, C03005, doi:10.1029/2004JC002398.

Bromirski, P.D., R.E. Flick, and D.R. Cayan, 2003: Decadal storminess variability along the California coast: 1858 - 2000, *J. Clim.*, **16**, 982-993.

Cazenave, A., and R. S. Nerem, 2004: Present-day sea level change: Observations and causes, *Rev. Geophys.*, **42**, RG3001, doi:10.1029/2003RG000139

Chelton, D. B., and R. E. Davis, 1982: Monthly mean seal-level variability along the west coast of North America. *J. Phys. Oceanogr.* **12**, 757-784.

Church J. A., J. M. Gregory, P. Huybrechts, M. Kuhn, K. Lambeck, M. T. Nhuan, D. Qin and P. L. Woodworth, 2001: Changes in sea level. Chapter 11 of the *Intergovernmental Panel on Climate Change Third Assessment Report.* Cambridge University Press, Cambridge, pp. 639-694.

Delworth, T. et al., 2006: GFDL's CM2 global coupled climate models - Part 1: Formulation and simulation characteristics. *J. Climate*, 19(5), 643-674.

Fairbanks, R. G., 1989: A 17,000-year Glacio-eustatic Sea Level Record: Influence of Glacial Melting Rates on the Younger Dryas Event and Deep-Ocean Circulation. *Nature* 342, no. 6250, p. 637-642.

Flick, R. E., 2000: Time-of-Day of Peak Tides in a Mixed-Tide Regime. *Shore & Beach,* **68**(4), 15-17.

Flick, R. E. and A. Badan-Dangon, 1989: Coastal Sea Levels During the January 1988 Storm off the Californias. *Shore and Beach,* **57**(4), 28-31.

Flick, R. E., 1998: Comparison of California tides, storm surges, and mean sea level during the El Niño winters of 1982–1983 and 1997–1998. *Shore and Beach,* **66**(3), 7-11.

Flick, R.E., J.F. Murray and L.C. Ewing, 2003: Trends in United States Tidal Datum Statistics and Tide Range, *J. Waterway, Port, Coastal and Ocean Eng*., Amer. Soc. Civil Eng., **129**(4), 155-164.

Hansen, J., 2005: Earth's Energy Imbalance: Confirmation and Implications. *Science* **308**(5727): 1431-1435.

Hulme, M., S. C. B. Raper, and T. M. L. Wigley, 1995: An integrated framework to address climate change (ESCAPE) and further developments of the global and regional climate modules (MAGICC). *Energy Policy,* **23**, 347-355.

Kalnay, E., M. Kanamitsu, R. Kistler, W. Collins, D. Deaven, L. Gandin, M. Iredell, S. Saha, G. White, J. Woollen, Y. Zhu, A. Leetmaa, B. Reynolds, M. Chelliah, W. Ebisuzaki, W. Higgins, J. Janowiak, K.C. Mo, C. Ropelewski, J. Wang, R. Jenne, and D. Joseph, 1996: The NCEP/NCAR 40-Year Reanalysis Project. *Bull. Amer. Meteor. Soc.,* **77**, 437 – 471.

Meehl, Gerald A. et al., 2005: How Much More Global Warming and Sea Level Rise? *Science* **307**(5716), 1769-1772.

Munk, W. H., and D. E. Cartwright, 1966: Tidal spectroscopy and prediction. *Phil. Trans. Roy. Soc. London*, **259**, 533-581.

Munk, W. H., 2002: "Twentieth century sea level: An enigma." *Proc. Nat. Acad. Sci.* 99(10), 6550-6555.

Ryan, H., H. Gibbons, J. W. Hendley, and P. Stauffer, 2000: El Niño sea-level rise wreaks havoc in California's San Francisco Bay Region. USGS Fact Sheet 175-99. Available online at: http://geopubs.wr.usgs.gov/fact-sheet/fs175-99/ .

Seymour, R.J., Strange, R.R., Cayan, D.R., and Nathan, R.A., 1984: Influence of El Niños on California's wave climate: *in* Proceedings of the 19th Coastal Engineering Conference: American Society of Civil Engineers. v. 1, p. 577–592.

Seymour, R.J., 1998: Effects of El Niños on the west coast wave climate: *Shore and Beach*, **66**(3), p. 3–6.

Storlazzi, C.D., and Griggs, G.B., 1998: The 1997–98 El Niño and erosion processes along the central coast of California: *Shore and Beach*, **66**(3), p. 12–17.

Trenberth, K., and J. Hurrell, 1994: Decadal atmosphere-ocean variations in the Pacific. *Climate Dynamics,* **9**, 303-319.

Wallace, J. M. and D. S. Gutzler, 1981: Teleconnections in the geopotential height field during the Northern-Hemisphere winter. *Mon. Wea. Rev.*, **109**, 784-812.

Washington, W. M., Weatherly, J. W., Meehl, G. A., Semtner, A. J., Bettge, T. W., Craig, A. P., Strand, W. G., Arblaster, J., Wayland, V. B., James, R. & Zhang, Y., 2000: Parallel Climate Model (PCM) control and transient simulations'. *Clim. Dyn.* **16**(10/11), 755–774.

Wigley, T. M. L., 2005: The Climate Change Commitment. *Science*, **307**, 1766-1769.

Zetler, D. B., and R. E. Flick, 1985: Predicted extreme high tides for mixed tidal regimes. *J. Phys. Oceanogr,* **15**(3), 357-359.

Table 1: Observed High Sea Level Occurrences from San Francisco and La Jolla Tide Gauge Records. Number of exceedances above 99.99th percentile thresholds from 1933-2004 hourly observations. Maximum values are relative to mean sea level.

San Francisco   99.99th percentile=141 cm   La Jolla (Scripps Pier) 99.99th percentile=141.2 cm

	San Fran			La Jolla		
	# > 99.99th	Max s.l. (m)	No. obs	# > 99.99th	Max s.l. (m)	No. obs.
1915 – 1933	1	1.43427	157798			
1933 – 1951	5	1.44627	157776	0	1.31815	148375
1951 – 1969	7	1.45627	157137	3	1.47315	144392
1969 – 1987	36	1.80027	155396	29	1.52515	145562
1987 - 2004	29	1.68027	149016	24	1.54615	148320

Table 2: Projected global sea level rise, in cm, relative to historical mean sea level, for the SRES A1fi, A2 and B1 scenarios as estimated by the latest AOGCM simulations combined with MAGICC projections for the ice melt component and the A1fi scenario.

	B1			A2			A1fi		
	Lo	med	Hi	Lo	Med	hi	lo	Med	Hi
1971-2000	-0.5	-0.2	0.4	-0.5	-0.2	0.3	-0.5	-0.1	0.4
2035-2064	6.0	14.9	31.1	6.3	15.1	28.8	7.1	16.9	32.2
2070-2099	10.9	26.4	53.9	14.2	32.8	60.5	16.8	38.7	71.6

Table 3: Linear regression model of non-tide sea level residuals based on Reanalysis and Nino 3.4 input as predictors of daily sea level, 1950-2002. Model coefficients and correlation with non-tide residuals, 1950-2002. *b)* Correlation between seasonal (Nov-Mar) non-tide residuals and ENSO indexfrom NINO 3.4 SSTs. τ_y and τ_y are west-to east and south-to-north wind stress components, respectively.

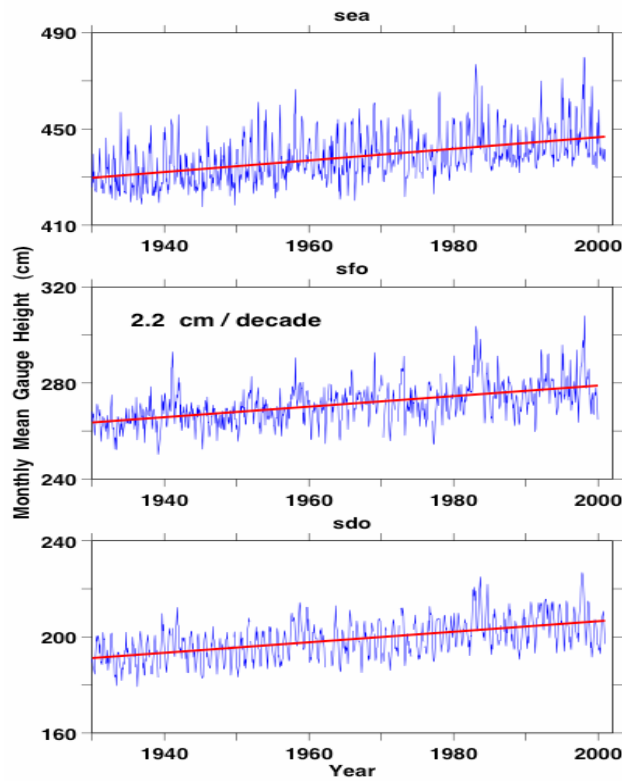| a)	Regression Coefficients				Goodness of fit			b) R non-tide s.l. vs. Nino 3.4
	SLP	τ_x	τ_y	Nino 3.4	R	Σ obs	σ model	
Cres City	1.61	-0.02	0.04	3.61	0.82	17.2	14.2	0.66
San Fran	1.37	0.01	0.04	5.33	0.79	12.3	9.7	0.75
La Jolla	1.15	-0.03	0.02	5.49	0.67	8.6	5.7	0.85

Table 4: Modeled San Francisco Sea Level exceedances occurring with prescribed mean sea level trend. 99.99% threshold 141cm, is from observed 1960-1978 hourly data at San Francisco. Trend's are linear from 2000 to 2100 weather and ENSO impact in sea level simulations from *the* GFDL CM2.1 A2 emissions scenario.

GFDL A2			
Trend cm/100 yr	2005-2034 99.99%	2035-2064 99.99%	2070-2099 99.99%
0	15	27	23
10	19	61	57
20	24	112	156
30	39	205	529
40	63	380	1470
50	97	679	3553
60	139	1238	7072
70	209	2152	12674
80	306	3455	20232

Table 5. Number of occurrences of hourly sea level events above historical 99.99 percentile at San Francisco, where sea level is rising at 30cm per century, with: a) tides, trend, weather and ENSO;   b) tides, trend, ENSO; and c) tides and trend. ENSO and weather- related sea level component are from GFDL A2 simulation.

GFDL A2 30cm Trend Model Components	2005-2034	2035-2064	2070-2099
Tides, trend, weather, ENSO	39	205	529
Tides, trend, ENSO	1	6	251
Tides, trend,	0	1	142

Figure 1: Observed monthly mean sea level (cm) from Seattle, San Francisco, San Diego tide gages.
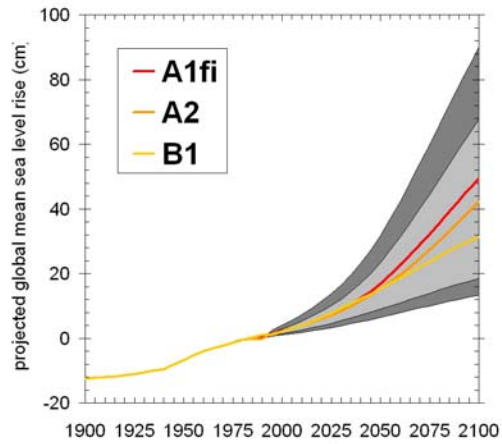

Figure 2: MAGICC-simulated relationship between the relative contributions of ice melt and thermal expansion to global sea level rise estimates over the next century, corresponding to the range of historical ratios derived from observational and modeling studies.
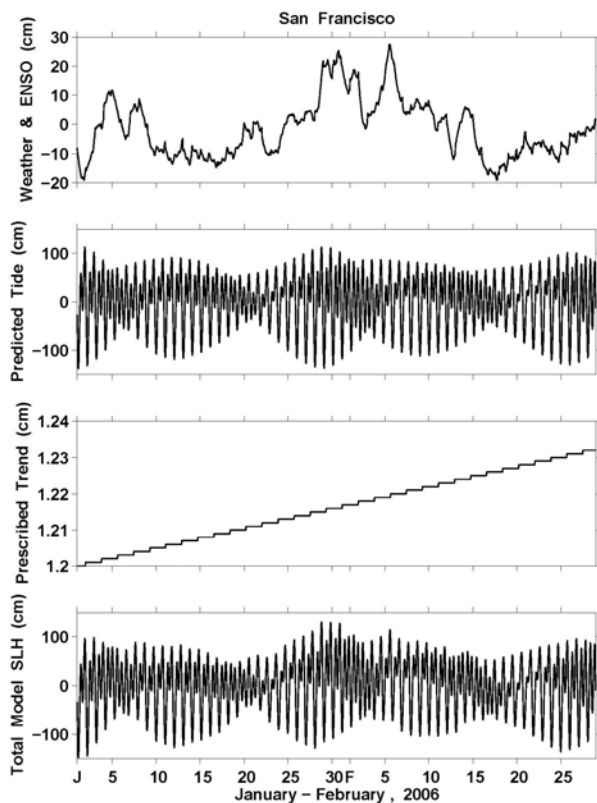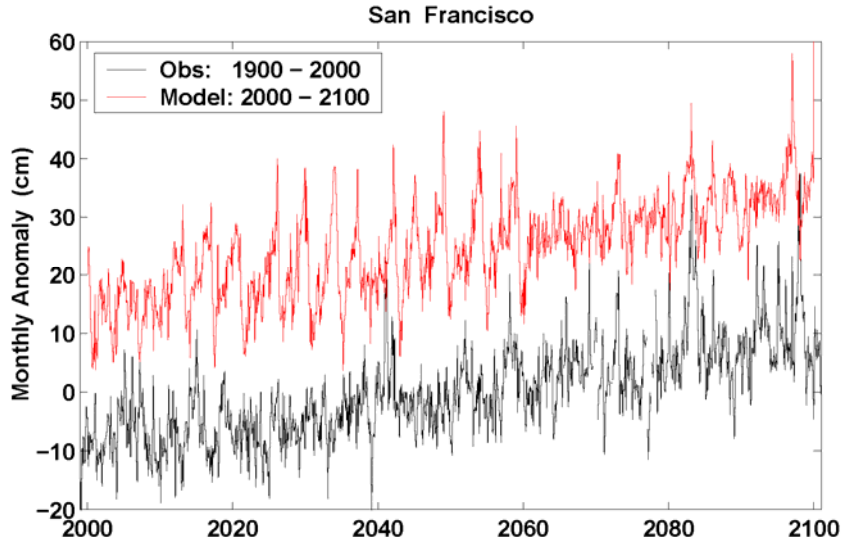
Figure 3: Projected sea level rise from climate model estimates for three GHG emissions scenarios, A1fi (high emissions), A2 (medium-high emissions) and B1 (low emissions).
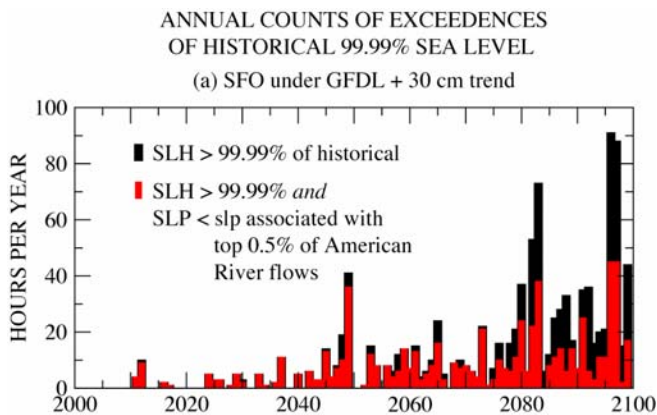

Figure 4: Modeled sea level, including non-tide, astronomical tide-prediction, linear trend (20 cm/year), and total sea level, January-February 2006.
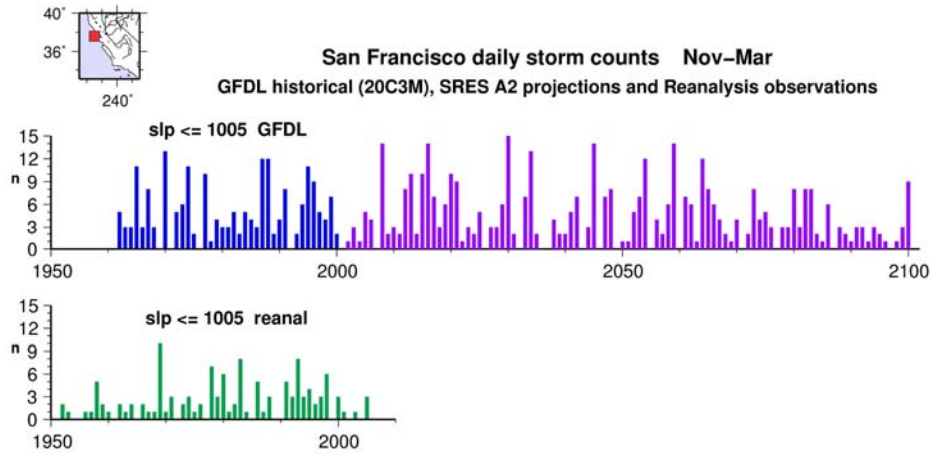
Figure 5: Model projected (red) monthly San Francisco sea level anomalies from mean sea level, for 2000-2100 from GFDL A2 model input with linear trend amounting to 20cm increase, 2000-2100. Observed (black) monthly sea level from San Francisco tide gage (1900-2100) is shown for comparison.
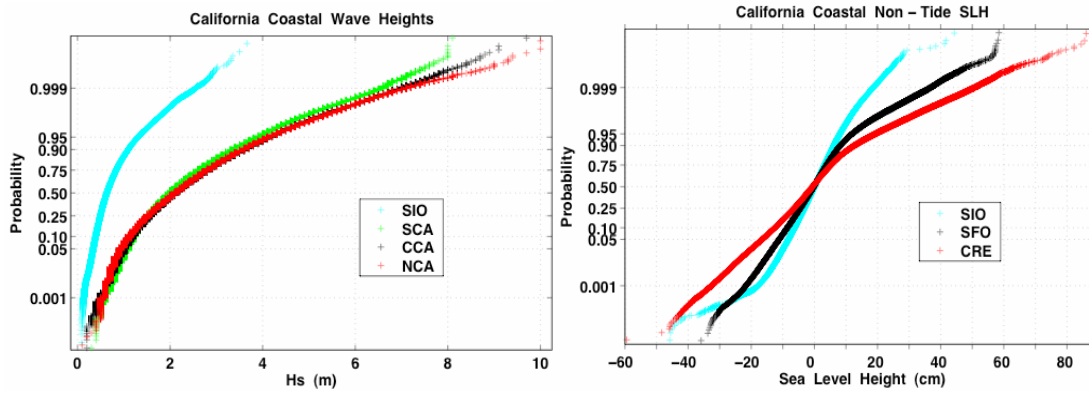

San Francisco

Figure 6: Projected total exceedances of San Francisco hourly sea level height (SLH) above historical 99.99 percentile (black), and number that are coincident with sea level pressure anomalies less than -4mb. Projected sea level from GFDL model weather and Nino3.4 SST with a linear trend of 30cm over 2000-2100.

ANNUAL COUNTS OF EXCEEDENCES
OF HISTORICAL 99.99% SEA LEVEL

(a) SFO under GFDL + 30 cm trend

Figure 7: Number of days per year of events with SLP is 1005 HPa or lower in vicinity of San Francisco from GFDL A2 simulation 1962-2100 (upper), and from NCEP/NCAR Reanalysis 1950-2004 (lower).

Figure 8: (left): normal (Guassian) cumulative probability distributions for hourly significant wave height near San Diego (SIO), Pt. Conception (SCA), San Francisco (CCA), and Crescent City (NCA). (right) Normal (Guassian) probability distributions for hourly non-tide sea levels at La Jolla (SIO), San Francisco (SFO), and Crescent City (CRE).

Figure 9: Association of Wave significant wave heights (Hs) at central California coastal buoys with non-tidal sea level anomalies at San Francisco. Each curve represents the conditional probability of Hs during a storm event characterized by non-tidal levels exceeding selected thresholds.